

The Effect of Molecular Orientation on the Potential of Porphyrin–Metal Contacts

Maxim P. Nikiforov,^{*,†} Ulrich Zerweck,[‡] Peter Milde,[‡] Christian Loppacher,[‡] Tae-Hong Park,[§] H. Tetsuo Uyeda,[§] Michael J. Therien,[§] Lukas Eng,[‡] and Dawn Bonnell[†]

Department of Materials Science and Engineering, Department of Chemistry, University of Pennsylvania, Philadelphia, Pennsylvania 19104-6323, and Institute of Applied Photophysics, Dresden University of Technology, Dresden, Germany

Received August 28, 2007; Revised Manuscript Received November 5, 2007

ABSTRACT

The effect of molecular orientation at metal contacts on interface properties was determined by examining the local work function of porphyrin on atomically smooth graphite. The orientation was varied by self-assembly from the vapor phase, and the local potential was quantified by Kelvin force microscopy (scanning surface potential microscopy). When the porphyrin ring is oriented parallel to the substrate, the surface work function is 50 mV less than that of the highly ordered pyrolytic graphite; in contrast, when the porphyrin molecular plane is oriented perpendicular to the substrate, the surface work function is unchanged. The orientation dependence of the surface work function is determined by the geometric relationships between the delocalized charge densities in the molecule and substrate and possible interface bonding. The differences in interface properties with molecular configuration have important design implications to molecular electronic and organic electronic devices.

The development of classes of organic compounds with unusual electronic and optical properties portends successful applications of these species in molecular electronics, electroluminescent devices, solar cells, photonics, and novel electro-optic materials. It is understood that for many of these applications, interfaces with electrodes are critical,¹ as these junctions will dictate the viability and performance of organic electronic devices.² Approaches used currently to characterize the device properties of molecules, such as break junctions,³ electromigrated junctions,⁴ and in-wire molecular junctions,⁵ neither control nor reveal the orientations of the molecules. To probe the importance of molecular orientation, we examine a model system in which the positional arrangement of a functional organic molecule at a metallic contact is varied by self-assembly and the local potential is directly probed. Work-function changes at organic molecule–contact interfaces that have been extensively studied for the past decade can be tuned by the length of organic molecule,^{6,7} by donor ability of the substituent,⁸ etc.⁹ However, we believe that this is the first direct correlation between molecular

orientation and potential at an electrode that is accomplished in a configuration representative of device interfaces.

Porphyrin compounds have been of interest for many years due to the facile ability to engender and tune optical and electrical functionality by varying the nature of the porphyrin ring central metal ion and modulating porphyrin σ - and π -system electronic structure through introduction of appropriate substituents at the macrocycle β - or meso-positions.¹⁰ Many substituted porphyrin systems have been established to self-assemble on metal surfaces.¹¹ The present study examines the interactions of 5,15-bis(2',6'-bis(3,3-dimethyl-1-butyloxy)phenyl)porphyrin (compound **1**)¹² with an atomically smooth graphite substrate, using noncontact-atomic force microscopy (nc-AFM) and Kelvin force microscopy (KFM, also referred to as scanning surface potential microscopy), to probe respectively structure and potential. We find that the orientation of the porphyrin at the electrode has a significant effect on the surface work function.

Compound **1** was synthesized using literature methods¹² and purified by several recrystallizations from hot hexane prior to vacuum deposition. A crystal of **1** suitable for X-ray structural analysis was obtained by slow evaporation of a CH₂Cl₂ solution. The compound **1** structure is illustrated in Figure 1. Note that the steric interaction between the porphyrin β -hydrogen and the 5- and 15-phenyl ring ortho-

* Corresponding author. E-mail: maximn@seas.upenn.edu.

[†] Department of Materials Science and Engineering, University of Pennsylvania.

[‡] Dresden University of Technology.

[§] Department of Chemistry, University of Pennsylvania.

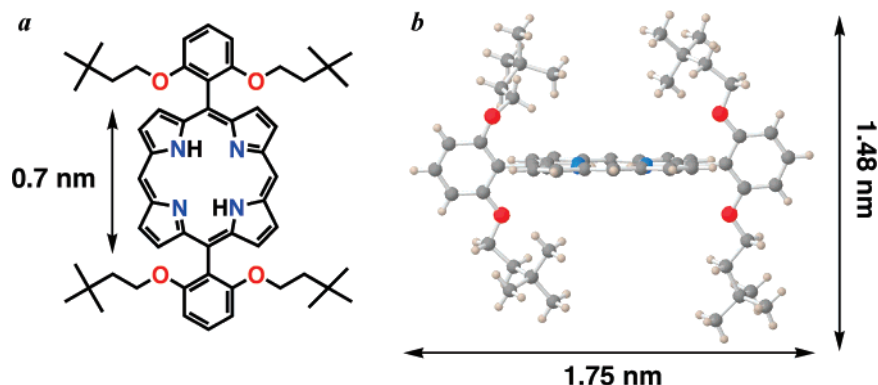


Figure 1. Compound **1** chemical structure (a); Compound **1** crystal structure (see Supporting Information) with key molecular dimensions highlighted (b).

oxygen atoms is substantial and severely restricts the extent of aryl ring vibrational motion as well as the range of accessible torsional angles between the phenyl and porphyrin least-squares planes at ambient temperature. Congruent with this fact, the observed torsional angle between the 5- and 15-aryl rings and the porphyrin plane is $\sim 70^\circ$ (Supporting Information), forcing the phenyl 2',6'-bis-3,3-dimethyl-1-butoxy substituents to lie approximately orthogonal to the porphyrin plane (Figure 1b).

Vacuum deposition of compound **1** was accomplished by heating the solid in a crucible in ultrahigh vacuum to a temperature between 130–150 °C. The deposition rate in these experiments was ~ 0.03 monolayer/sec. A nominal thickness of about 1 monolayer of porphyrin was deposited on highly ordered pyrolytic graphite (HOPG); however, AFM studies demonstrated subsequently that submonolayer ($\sim 60\%$) coverage was realized. A commercial low-temperature AFM (Cryogenic SFM Omicron NanoTechnology GmbH), modified with home-built electronics, was used for nc-AFM and KFM measurements.¹³ The oscillation amplitude was maintained at 1.4 nm peak-to-peak; the oscillation phase remained constant. Frequency shifts from -15 to -200 Hz were used for imaging. Molecular resolution in nc-AFM is obtained when the oscillating tip interacts with the force field within bonding distances with the surface.¹⁴ Silicon tips (Super Sharp Silicon probes from NanoWorld AG (Switzerland)) coated with 1 nm of Cr, prepared in-house, were used for nc-AFM and KFM measurements. The cantilever resonant frequency was 180 kHz. All measurements were carried out at pressures below 1×10^{-10} mBar at 80 K.

The deposition of a nominal monolayer of compound **1** on HOPG results in islands with 2 step heights: 0.6 and 1.55 nm (Figure 2). The height of step A corresponds to the width of the porphyrin ring (~ 0.7 nm), while that of step B matches the length spanned by the two 3,3-dimethyl-1-butoxy groups, which lie above and below the porphyrin plane (Figure 1b). Note that the height precision in this measurement (~ 0.2 nm) is sufficient to distinguish between multiple porphyrin layers and intermediate values, in this case the difference between 1.2 and 1.4 nm for double layers and 1.55 nm. Furthermore, the lateral structure is consistent with this assignment.

Both types of monolayers assemble into laterally ordered structures; Figure 3 compares molecular resolution nc-AFM topographic images of the two surface structures. The lattice parameters of structure A, determined by taking fast Fourier transformation of the Figure 3a data, are $a_1 = 1.79$ nm and $a_2 = 1.55$ nm with a 101° angle between the vectors and a corrugation amplitude of 0.05 nm. The in-plane lattice parameters of the porphyrin monolayer that defines island A are close to the molecular dimensions highlighted in Figure 1b. Taking into account a ~ 0.7 nm step height, it is logical to assume that the porphyrin rings of island A are oriented perpendicular to the substrate (Figure 2e) superposition of the molecular structure oriented to match the lattice dimensions, and the topographic contrast is shown in Figure 3a, resulting in molecular surface concentration on Step A of $3.67 \times 10^{17}/\text{m}^2$. This configuration attributes the bright contrast to the compound **1** phenyl and porphyrin rings and the gray background to the 2',6'-alkoxy groups. While the structure is periodic, there is some variation in the lateral dimensions. A rigid translation of the lattice superimposes exactly on the image contrast over about 90% of the area; about 10% of the structure appears to be somewhat expanded or contain isolated defects. The structure of island B is similarly determined from Figure 3c; here in-plane lattice parameters are $a_1 = 1.15$ nm and $a_2 = 1.29$ nm with a 97° angle between the vectors and a corrugation amplitude of 0.05 nm, resulting in molecular surface concentration on Step B of $6.79 \times 10^{17}/\text{m}^2$. On the basis of the lattice parameters of the monolayer obtained from Figure 3c and the fact that the porphyrin ring on island B lies parallel to the substrate from Figure 2e (determined from the step height), the molecular orientation of Figure 3d is proposed. Note in this case that the phenyl rings are situated at the highest contrast because the 2',6'-bis(3,3-dimethyl-1-butoxy) substituents extend above them (see Figure 1). The structures proposed for the A and B islands are similar to the “face-on”^{15,16} and “edge-on”¹⁶ stacking modes of porphyrin molecules observed in monolayers and the solid state. The nc-AFM contrast can derive from variations in the local electronic structure, the geometric structure, and/or the rigidity within the molecule. The experiments do not determine the mechanism of contrast formation; however, all three contrast formation mechanisms

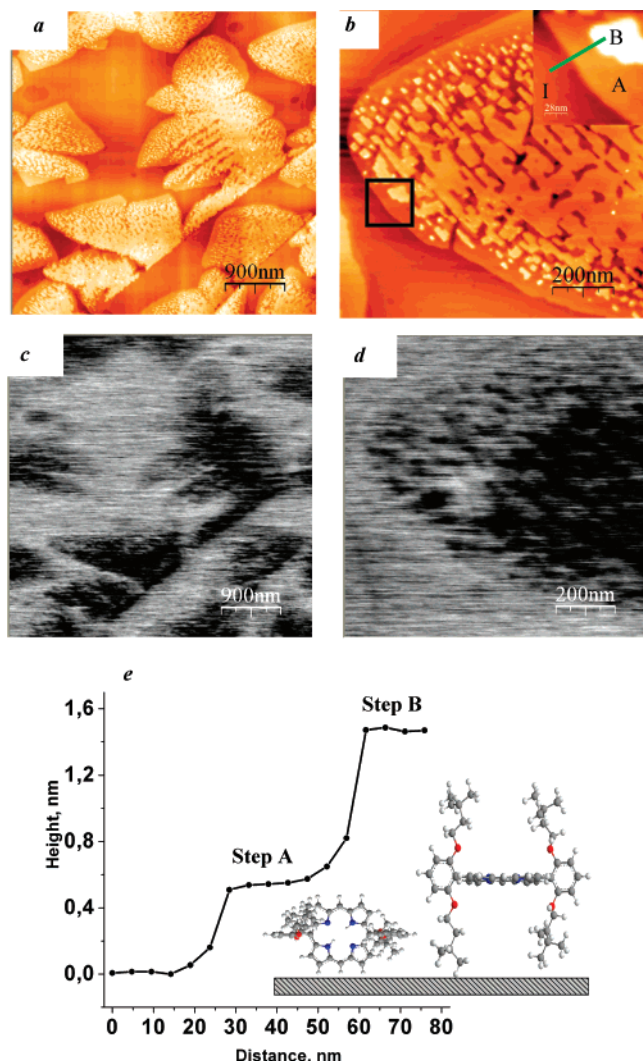


Figure 2. nc-AFM images of compound **1** deposited on a HOPG surface at different magnifications (a,b) with KFM images of the same area (c,d). The inset of panel b shows detail in a region identified by the box. The line profile from the inset is presented in (e). Region I corresponds to the HOPG, and regions A and B correspond to porphyrin monolayers that vary with respect to the observed island step height. Black-to-white contrast in surface potential images is 100 mV, resonant frequency of the tip = 180 kHz, frequency shift = −150 Hz. Measurements were done at 80 K.

result in the same image pattern with varying corrugation amplitudes. To relate these structures to interface properties, KFM and nc-AFM were performed simultaneously (Figure 2c,d). Variations in surface potential are correlated with the location and nature of the compound **1** monolayers. The difference between the potential of island A and that of the graphite substrate was below the energy resolution limit (~ 5 meV). The island A surface potential ($V_{\text{step A}} = 0.64$ eV) is 50 meV greater than that determined for island B ($V_{\text{step B}} = 0.59$ eV), which is an order of magnitude larger than the energy resolution limit. Note that while the absolute values of surface potential are difficult to extract from KFM, differences in potential are highly accurate.^{13,17}

The difference in the work functions of metallic chromium (IE = -4.5 ± 0.4 eV) and graphite (IE = -5.0 ± 0.4 eV)

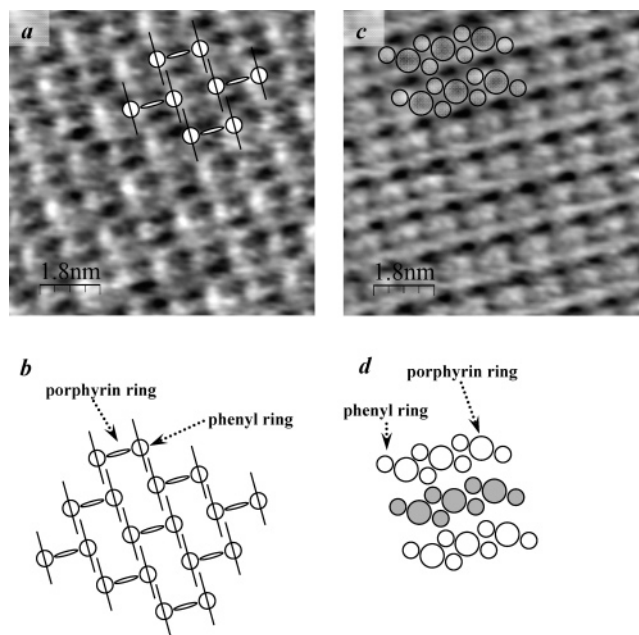


Figure 3. High-resolution nc-AFM topographic images of island A (a) and B (c) illustrate the molecular structure on the 9 nm length scale. Arrangements of compound **1** molecules within islands A (b) and B (d) are shown schematically in (c) and (d). Resonant frequency of the tip = 180 kHz, frequency shift = −150 Hz, Black-to-white contrast is 0.04 nm (a), 0.05 nm (c). Measurements were carried out at 80 K.

corresponds quantitatively to the measured surface potential (0.64 ± 0.01 eV) (Figure 4). A comparison of Figure 2 and Figure 4 shows that the porphyrin oriented with the ring perpendicular to the surface does not alter measurably the work function of the electrode; in contrast, when compound **1** is oriented with the ring parallel to the surface, the vacuum level lowers by 50 meV. Figure 4 illustrates the electrostatic effect of molecular orientation in terms of local charge distribution. The π -symmetric orbitals of the porphyrin and underlying substrate facilitate charge delocalization. When oriented parallel to the surface, the porphyrin ring area is equivalent to that of ~ 7 graphite hexagons; the 18π electron porphyrin aromatic ring therefore resides 0.7 nm above 10π electron delocalized graphite system, resulting in dipole moment of 8.96×10^{-28} C·m (~ 105 Debye). The work function change (ΔE) linked to the dipole moment perpendicular to the interface (μ) through the equation $\Delta E = e \cdot \Gamma \cdot \mu / \epsilon_0 \epsilon$,¹⁸ where e is the electron charge (1.6×10^{-19} C), Γ is the molecular surface concentration ($6.79 \times 10^{17} \text{ m}^{-2}$ in case of Step B), ϵ_0 is the permittivity of free space ($8.85 \times 10^{-12} \text{ F} \cdot \text{m}^{-1}$), and ϵ is the relative dielectric constant (3 in the case of porphyrin).¹⁹ The change in work function $\Delta E = 50$ meV corresponds to an interfacial dipole between step B and HOPG of only 1.96×10^{-30} C·m (~ 0.7 Debye), implying that significant charge screening at porphyrin–HOPG interface occurs. When the charge density of the porphyrin lies perpendicular to the surface (left), the magnitude of the dipolar interaction is diminished greatly. These studies thus indicate that in a metal–porphyrin–metal device configuration, molecules oriented with the porphyrin ring parallel to the surface will demonstrate an increased hole injection

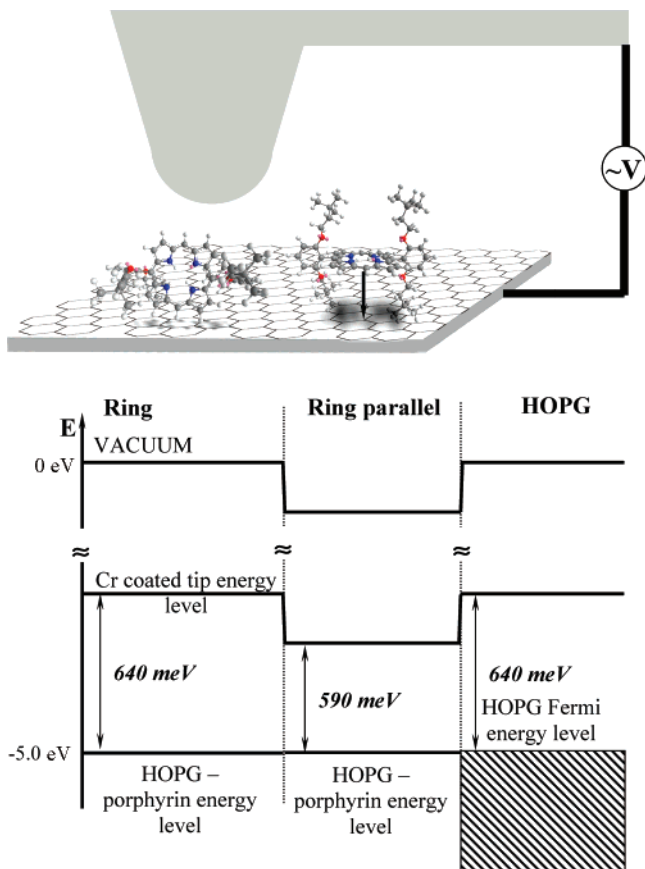


Figure 4. Schematic diagram illustrating the basis of the molecular orientation dependence of the measured surface potential for porphyrin on graphite. The delocalized charge density of compound **1** parallel to the surface (right) is separated from that of the substrate by 0.7 nm, creating a dipole. When the charge density of the porphyrin lies perpendicular to the surface (left), the magnitude of the dipolar interaction is diminished greatly.

barrier of 50 mV with respect to analogous structures oriented perpendicular to the surface. Macroscopic transport studies of porphyrin films show that metal–porphyrin contacts exhibit behavior between that of the Schottky–Mott and Bardeen-type limits.²⁰ However, in these and similar measurements the local order structure and orientations of the molecules at the interface are not known.²¹ In ref 22, the authors observed an interfacial dipole between porphyrin and a substrate, but pointed out that the origin of dipole formation remained unclear. Our results underscore the impact of molecular orientation upon dipole formation and, thus, thin film transport properties.

We have demonstrated that the work function of porphyrin monolayers on HOPG depends acutely on molecular orientation. This orientation dependence derives from the geometric relationship between the delocalized charge densities of the molecule and substrate and differences in the nature of interfacial bonding. This study demonstrates that when the porphyrin ring is oriented parallel to the substrate, the surface work function is 50 mV less than that of the HOPG; in contrast, when the porphyrin molecular plane is oriented perpendicular to the substrate the surface work function is

unchanged. As the molecule/electrode interface often dominates device properties, differences in surface potential that derive from molecular configuration have important implications to molecular and organic electronics.

Acknowledgment. The authors gratefully acknowledge financial support from the Nano/Bio Interface Center at the University of Pennsylvania (DMR04–25780) and MRSEC (DMR05–20020) funded by the National Science Foundation and the SFB 287 funded by the German Science Foundation. The structure of compound **1** was determined by Dr. Patrick Carroll (X-ray Facility, Department of Chemistry, University of Pennsylvania).

Supporting Information Available: An X-ray crystallographic file (CIF format), an ORTEP diagram, tables of crystal data, structure solution and refinement, atomic coordinates, bond lengths and angles, and anisotropic thermal parameters for compound **1**. This material is available free of charge via the Internet at <http://pubs.acs.org>.

References

- (1) Fahlman, M.; Crispin, A.; Crispin, X.; et al. *J. Phys.: Condens. Matter* **2007**, *19* (18), 183202.
- (2) Koch, N. *ChemPhysChem* **2007**, *8* (10), 1438.
- (3) Reed, M. A.; Zhou, C.; Muller, C. J.; et al. *Science* **1997**, *278* (5336), 252.
- (4) Strachan, D. R.; Smith, D. E.; Johnston, D. E.; et al. *Appl. Phys. Lett.* **2005**, *86* (4), 043109.
- (5) Cai, L. T.; Cabassi, M. A.; Yoon, H.; et al. *Nano Lett.* **2005**, *5* (12), 2365.
- (6) Zehner, R. W.; Parsons, B. F.; Hsung, R. P.; et al. *Langmuir* **1999**, *15* (4), 1121.
- (7) Lu, J.; Eng, L.; Bennewitz, R.; et al. *Surf. Interface Anal.* **1999**, *27* (5–6), 368.
- (8) Koh, S. E.; McDonald, K. D.; Holt, D. H.; et al. *Langmuir* **2006**, *22* (14), 6249.
- (9) Zuppiroli, L.; Si-Ahmed, L.; Kamaras, K.; et al. *Eur. Phys. J. B* **1999**, *11* (3), 505.
- (10) Dolphin, D. *The Porphyrins*; Academic Press: New York, 1978.
- (11) (a) Scudiero, L.; Barlow, D. E.; Hipps, K. W. *J. Phys. Chem. B* **2002**, *106* (5), 996. (b) Scudiero, L.; Barlow, D. E.; Mazur, U.; et al. *J. Am. Chem. Soc.* **2001**, *123* (17), 4073.
- (12) Uyeda, H. T.; Zhao, Y. X.; Wostyn, K.; et al. *J. Am. Chem. Soc.* **2002**, *124* (46), 13806.
- (13) Zerweck, U.; Loppacher, C.; Otto, T.; et al. *Phys. Rev. B* **2005**, *71* (12), 125424.
- (14) Nikiforov, M. P.; Bonnell, D. A. In *Science of Microscopy*; Hawkes, P. W., Spence, J. C. H., eds.; Springer: New York, 2007; p 1400.
- (15) (a) Otsuki, J.; Nagamine, E.; Kondo, T.; et al. *J. Am. Chem. Soc.* **2005**, *127* (29), 10400. (b) Terui, T.; Kamikado, T.; Okuno, Y.; et al. *Curr. Appl. Phys.* **2004**, *4* (2–4), 148. (c) Ogunrinde, A.; Hipps, K. W.; Scudiero, L. *Langmuir* **2006**, *22* (13), 5697.
- (16) Zhou, Y. S.; Wang, B.; Zhu, M. Z.; et al. *Chem. Phys. Lett.* **2005**, *403* (1–3), 140.
- (17) Kalinin, S. V.; Bonnell, D. A. *Phys. Rev. B* **2004**, *70* (23), 235304.
- (18) Kronik, L.; Shapira, Y. *Surf. Sci. Rep.* **1999**, *37* (1–5), 1.
- (19) Visseu, T. M. R.; Hungerford, G.; Ferreira, M. I. C. *J. Phys. Chem. B* **2002**, *106* (8), 1853.
- (20) Ishii, H.; Sugiyama, K.; Yoshimura, D.; et al. *IEEE J. Sel. Top. Quantum Electron.* **1998**, *4* (1), 24.
- (21) Koch, N.; Salzmann, I.; Johnson, R. L.; et al. *Org. Electron.* **2006**, *7* (6), 537.
- (22) Molodtsova, O. V.; Schwieger, T.; Knupfer, M. *Appl. Surf. Sci.* **2005**, *252* (1), 143.

NL072175D